Solar Phys (2008) 249: 281–291
DOI 10.1007/s11207-008-9187-7

The High-Resolution Solar Reference Spectrum between 250 and 550 nm and its Application to Measurements with the Ozone Monitoring Instrument

Marcel Dobber · Robert Voors · Ruud Dirksen · Quintus Kleipool · Pieternel Levelt

Received: 13 December 2006 / Accepted: 4 April 2008 / Published online: 16 May 2008

Abstract We have constructed a new high resolution solar reference spectrum in the spectral range between 250 and 550 nm. The primary use of this spectrum is for the calibration of the Dutch – Finnish Ozone Monitoring Instrument (OMI), but other applications are mentioned. The incentive for deriving a new high resolution solar reference spectrum is that available spectra do not meet our requirements on radiometric accuracy or spectral resolution. In this paper we explain the steps involved in constructing the new spectrum, based on available low and high resolution spectra and discuss the main sources of uncertainty. We compare the result with solar measurements obtained with the OMI as well as with other UV-VIS space-borne spectrometers with a similar spectral resolution. We obtain excellent agreement with the OMI measurements, which indicates that both the newly derived solar reference spectrum and our characterization of the OMI instrument are well understood. We also find good agreement with previously published low resolution spectra. The absolute intensity scale, wavelength calibration and representation of the strength of the Fraunhofer lines have been investigated and optimized to obtain the resulting high resolution solar reference spectrum.

Keywords OMI: Ozone Monitoring Instrument · GOME: Global Ozone Monitoring Experiment · SCIAMACHY: SCanning Imaging Absorption spectroMeter for Atmospheric CHartographY

1. Introduction

A spectrum of the Sun has many potential applications, most notably in studies of the climate and of the Sun itself. Much less is known about the spectral structure than the integrated irradiance of the Sun's spectrum. An accurate solar spectrum is needed, *e.g.*, in the radiative transfer calculation of the Earth's atmosphere. In this paper, our main objective for producing a spectrally and radiometrically calibrated high resolution solar reference spectrum in

M. Dobber (✉) · R. Voors · R. Dirksen · Q. Kleipool · P. Levelt
KNMI/Royal Netherlands Meteorological Institute, PO Box 201 3730 AE De Bilt, Netherlands
e-mail: dobber@knmi.nl

the UV-VIS spectral range is to provide a reference for the study of the Earth's atmosphere, in particular within the framework of EOS-Aura's Dutch – Finnish Ozone Monitoring Instrument (OMI). OMI is a UV-VIS (270 – 500 nm) nadir viewing spectrometer at medium resolution (∼ 0.5 nm) aboard the EOS-Aura satellite, launched on 15 July 2004 (Dobber *et al.*, 2006; Levelt *et al.*, 2006a; Schoeberl *et al.*, 2006). The OMI contributes to EOS-Aura's main mission objectives: to observe the Earth's atmosphere in order to answer questions concerning the possible recovery of the ozone layer, air quality (*e.g.*, pollution) and climate change (Levelt *et al.*, 2006b). The OMI obtains measurements of the radiation backscattered from the Earth's surface and atmosphere as well as daily measurements of the Sun. For the Earth measurements the OMI has a wide instantaneous field-of-view perpendicular to the flight direction. In the Sun-synchronous polar orbit, this results in a daily global coverage, with a nadir footprint of 13 km × 24 km. The OMI measurements are used to study a number of atmospheric trace gases, such as ozone and NO_2, as well as aerosols and clouds. The OMI follows in the footsteps of previous instruments that observed the Earth's atmosphere in the UV-VIS, like the Total Ozone Mapping Spectrometer (TOMS, Heath and Park, 1978), the Solar Backscatter Ultraviolet instrument (SBUV, Heath and Park, 1978), the Global Ozone Monitoring Instrument (GOME, Burrows *et al.*, 1999) and the SCanning Imaging Absorption spectroMeter for Atmospheric CHartographY (SCIAMACHY, Burrows *et al.*, 1995).

A high resolution solar reference spectrum has many potential applications. For the OMI we identify two main areas of interest. First, the wavelength calibration of the OMI spectra: this is based on fitting Fraunhofer absorption lines in both the irradiance and the radiance spectra. We obtain the necessary solar spectrum at the OMI resolution by convolving a high resolution solar spectrum with the OMI instrument spectral response function (slit function). The latter was determined accurately on the ground by measurements made with a purpose-built instrument (Dirksen *et al.*, 2006). These measurements were made during the on-ground calibration campaign.

However, we found that the available solar reference spectra (Kurucz *et al.*, 1984; Hall and Anderson, 1991; Woods *et al.*, 1996; Chance and Spurr, 1997; Thuillier *et al.*, 1997, 1998, 2003) did not meet our requirements on spectral resolution and radiometric accuracy. For this reason a new radiometrically and spectrally calibrated high resolution solar reference spectrum has been constructed using both existing literature solar reference spectra and solar measurement data obtained with the OMI. For the second application in the OMI the solar reference spectrum is used to validate the radiometric calibration of the OMI measurements and to monitor potential optical degradation, since the solar spectrum itself at the UV-VIS wavelengths that the OMI measures is very stable. For this application the absolute radiometric accuracy of the solar reference spectrum with high spectral resolution needs to be in the order of 3 – 5% or better. For the OMI wavelength calibration and for the radiometric calibration the spectral resolution of the used high resolution solar reference spectrum needs to be at least an order of magnitude higher than the OMI spectral resolution, which amounts to about 0.4 – 0.6 nm.

The outline of the paper is as follows. First we provide a short overview of previously published solar reference spectra. We highlight their main properties and indicate why they do not meet our requirements. Next, we present a method for improvement by using the currently available literature spectra and solar measurement obtained with the OMI. Subsequently we present the finally obtained high resolution solar reference spectrum and we compare this spectrum with other existing spectra. We show that the high resolution spectrum convolved with the OMI slit function compares well with OMI measurements.

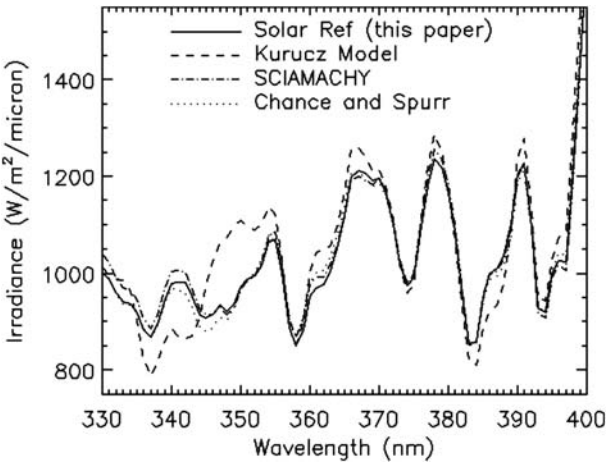

Figure 1 Comparison of four solar spectra at 2 nm resolution. The Kurucz model spectra show a relatively large difference while the other three spectra match much better.

2. Overview of Existing Solar Reference Spectra

Based on spectral resolution we can divide the existing solar reference spectra into two groups, spectra with low resolution above 0.1 nm full width at half maximum (FWHM) resolution and spectra with high resolution. This separation is based on the spectral resolution and sampling of OMI spectra. Our main use of the high resolution spectrum is to convolve it with OMI slit function, in order to obtain a spectrum at OMI resolution. For this, the spectral resolution of the input spectrum needs to be significantly higher than that of the desired target spectrum. An overview of all solar spectra discussed in this paper is given in Table 1.

Only a few high resolution solar spectra in the UV-VIS domain are available. One of the most widely used spectra is that of Chance and Spurr (1997). This is a composite of a high resolution UV-balloon spectrum, covering the wavelength range between 200 and 310 nm (Hall and Anderson, 1991) and ground based spectra obtained at Kitt Peak, covering the range between 296 and 1200 nm (Kurucz *et al.*, 1984). The accuracy of the wavelength scale is reported to be 0.002 nm below 300 nm and 0.001 nm above 305 nm. The combined spectrum is at 0.01 nm sampling and at 0.025 nm resolution.

High resolution solar reference spectra based on an accurate model of the Sun, such as those by Kurucz (1995), have a clear advantage over observed spectra because of the unlimited spectral coverage, sampling and resolution one can obtain. However, we found that the radiometric accuracy and more importantly the relative strength of many Fraunhofer lines in the spectrum did not match observations well enough (Figure 1).

Also for the lower resolution solar spectra a number of results are available. The SUSIM instrument on UARS measured in the UV spectral region (up to 410 nm) with a 0.15 nm spectral resolution (Floyd *et al.*, 2003). For the visible spectral region (400 nm and higher) a balloon spectrum was measured for the validation of the SCIAMACHY instrument on the ESA ENVISAT satellite (Gurlit *et al.*, 2005). A widely used low resolution solar reference spectrum based on observations is that of Thuillier *et al.* (2003). This spectrum, with a wavelength coverage between 200 and 2400 nm is also a composite spectrum, based on measurements with the satellite instruments SOLSPEC (Thuillier *et al.*, 1998) and SOSP (Thuillier *et al.*, 2003). Most of their effort has gone into ensuring excellent radiometric accuracy. The precise spectral resolution of the spectrum is not quoted. The SOLSPEC data (between 200 and 850 nm) were measured at 1 nm resolution and the Fraunhofer lines from Kurucz and Bell (1995) were installed at 1 nm resolution. For this reason we assume that

Table 1 Overview of referenced spectra in this paper. The primary input spectra used in this study to construct the radiometrically calibrated high resolution spectrum are indicated by an asterisk.

Spectrum name	Wavelength range (nm)	Spectral resolution (nm)	Spectral sampling (nm)	References
OMI	270 – 500	0.45 – 0.65	0.15 – 0.32	Levelt *et al.* (2006a, 2006b) Dobber *et al.* (2006)
SCIAMACHY	215 – 2380	0.24 – 1.5	0.1 – 0.8	Weber (2006)
SUSIM-UARS (*)	115 – 410	0.15	0.05	Floyd *et al.* (2003)
Thuillier	200 – 2400	1 (assumed, see text)	0.015 – 1	Thuillier *et al.* (2003)
Chance & Spurr (*)	200 – 1000	0.025	0.01	Chance and Spurr (1997)
Kitt Peak	296 – 1300	< 0.005	0.0003 – 0.001	Kurucz *et al.* (1984)
Hall & Anderson	200 – 310	~ 0.025	0.01	Hall and Anderson (1991)
VIS balloon (*)	315 – 650	0.55 – 1.48	0.1	Gurlit *et al.* (2005)

the spectral resolution (between 200 and 850 nm) is 1 nm, though most comparisons of this spectrum with known reference spectra were performed at 5 nm resolution. A list of high resolution and low resolution solar spectra is given in Table 1, along with their properties.

3. Method

In the previous section we indicated that none of the available spectra meet both our requirements on spectral resolution and radiometric accuracy simultaneously. In this section the method to construct a high resolution solar reference spectrum with sufficient radiometric accuracy is described. The method consists of four steps:

1. Convolve a high resolution spectrum with lower radiometric calibration accuracy with the best slit function that is available for the lower-resolution solar reference spectrum: $F_{\text{hires}} \otimes S_{\text{lores}} \Rightarrow F_{\text{lores}}^{\text{hisamp}}$.
2. Interpolate the thus obtained high sampling, low resolution spectrum on the wavelength grid of the low resolution reference spectrum: $\text{Regrid}(F_{\text{lores}}^{\text{hisamp}}) \Rightarrow F_{\text{lores}}^{\text{losamp}}$.
3. Divide that spectrum by the low resolution spectrum, to obtain the fraction by which to multiply the original high resolution spectrum, used in the first step: $F_{\text{lores}}^{\text{losamp}} / F_{\text{lores}}^{\text{meas}} \Rightarrow Q^{\text{losamp}}$.
4. Interpolate the fraction from 3 to the high resolution wavelength grid: $\text{Regrid}(Q^{\text{losamp}}) \Rightarrow Q^{\text{hisamp}}$.

The new high resolution solar reference spectrum is defined by $F_{\text{hires}}^{\text{REF}} \equiv Q^{\text{hisamp}} \cdot F_{\text{hires}}$.

Step 3 forms the basis of the method. It gives the difference between the absolute radiometric calibration of the original high resolution spectrum and the low resolution spectrum used as radiometric reference, as a function of wavelength. In step 4 this 'relative difference spectrum' is sampled at the same sampling as the original high resolution spectrum.

In the process of deriving the new radiometrically and spectrally calibrated high resolution solar reference spectrum the following points need to be considered carefully:

- The choice of the original high resolution spectrum that has a radiometric calibration with lower accuracy.

- The choice of the best lower resolution reference spectrum that has the best available radiometric calibration accuracy.
- How to determine the spectral response function (slit function) of the instrument that provides the low resolution reference spectrum.
- Important details of the interpolation process.
- Sources of uncertainty.

3.1. The Original High Resolution Spectrum

There is not a single high resolution spectrum that covers the entire wavelength range between 250 and 550 nm. The visible region is well observable from the ground, but the UV-region must be observed from space, because of the strong atmospheric absorption below 300 nm. Following the approach of Chance and Spurr (1997), we combine the UV spectrum of Hall and Anderson (1991), which covers the region between 200 and 310 nm and the ground-based ultra-high resolution spectrum obtained at Kitt Peak (Kurucz *et al.*, 1984).

The Kitt Peak spectrum was convolved with a triangular slit function with a FWHM of 0.025 nm, and sampled at 0.01 nm, to match the sampling and resolution and the instrument slit function of the UV spectrum. This merging revealed that the accuracy of the wavelength scale of the UV spectrum in the overlap region (between 296 and 303 nm) was on the order of the sampling, 0.01 nm. We expect the accuracy of the UV spectrum to be the same. The resulting accuracy of the wavelength scale was determined by Chance and Spurr (1997) to be better than 0.001 nm above 305 nm and 0.002 nm below 300 nm.

3.2. The Original Low Resolution Spectrum

As is the case for the high resolution reference spectrum, the low resolution spectrum is a composite of a number of contributions. For the UV spectral region (up to 410 nm) we used the 0.15 nm resolution SUSIM data set from UARS (Floyd *et al.*, 2003). We calculated the average of spectra spanning almost one complete solar cycle, from 1991 to 1999. For the visible spectral region (from 400 nm) we used the balloon spectrum obtained for the SCIAMACHY validation (Gurlit *et al.*, 2005). The radiometric calibration of the two spectra agrees to within 3% in the overlap wavelength range 400 – 412 nm. The wavelength calibration of the low resolution spectra was improved. We find that in order to match the wavelength calibration of the SUSIM spectra to that of the high resolution reference spectrum, shifts of ± 0.04 nm are necessary (Figure 2). This is in line with the 0.035 nm (2σ) wavelength accuracy quoted for the SUSIM UARS data (Woods *et al.*, 1996). We find that this wavelength update is very stable in time as can be seen from the small amount of scatter between the individual measurements, indicated by dots in Figure 2. The wavelength scale of the individual SUSIM spectra was improved before the average over the years 1991 to 1999 was calculated. Figure 3 shows the results of the wavelength scale analysis for the balloon spectrum of Gurlit *et al.* (2005). The main motivations for choosing the high resolution SUSIM data set from UARS (Floyd *et al.*, 2003) for the present work are the good spectral resolution, the good spectral sampling, the good spectral calibration and the good spectral stability of these spectra (see Figure 2) and a spectral slit function that turns out to be well behaved for our application (see Section 3.3). In addition, the SUSIM measurement series covers many years.

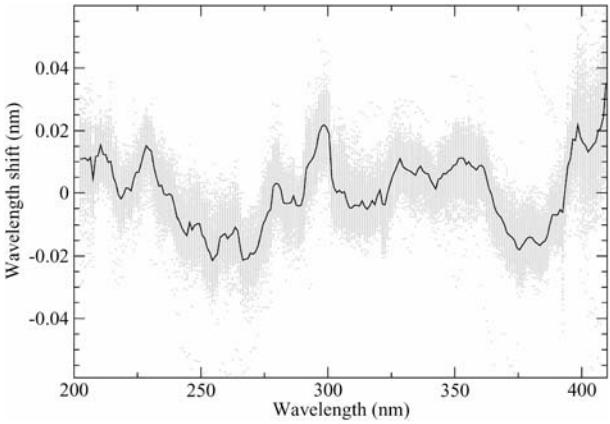

Figure 2 Wavelength correction made to the SUSIM 0.15 nm resolution spectra. The thick dark line is the result for the average, the small dots indicate each individual correction.

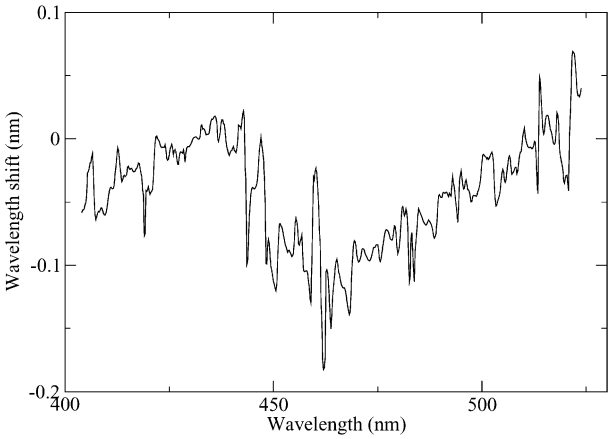

Figure 3 Wavelength correction made to the balloon spectrum of Gurlit *et al.* (2005).

3.3. The Instrument Spectral Response Function (Slit Function)

In order to match the high resolution spectra to the lower resolution spectra, the former need to be convolved with the instrument slit function of the lower resolution instrument. Unfortunately, these are not well known. However, from the technical description of the instruments, we can get a good first guess of the shape. The SUSIM instrument is equipped with a grating and scans across the detectors. This results in a triangular shape of the slit function (Brueckner *et al.*, 1993). The DOAS balloon spectrum is obtained by a non-scanning spectrograph, with a rectangular entrance slit with a width corresponding to that of five photodiode elements. This setup will result in a more square shaped slit function (Gurlit *et al.*, 2005). In Figure 4 the ratio of the convolution of the high resolution reference spectrum with the spectral slit function of the instrument that measured the low resolution spectrum and the measured low resolution spectrum is shown as a representative example for a limited wavelength range 400 – 440 nm for the DOAS balloon spectrum. The ratio shows both high-frequency features associated with the solar Fraunhofer lines and the spectral slit functions and lower-frequency features associated with radiometric calibration differences between the high resolution spectrum and the low resolution spectrum. Variation of the spectral slit function shape and width in order to obtain a result that has the least high-frequency struc-

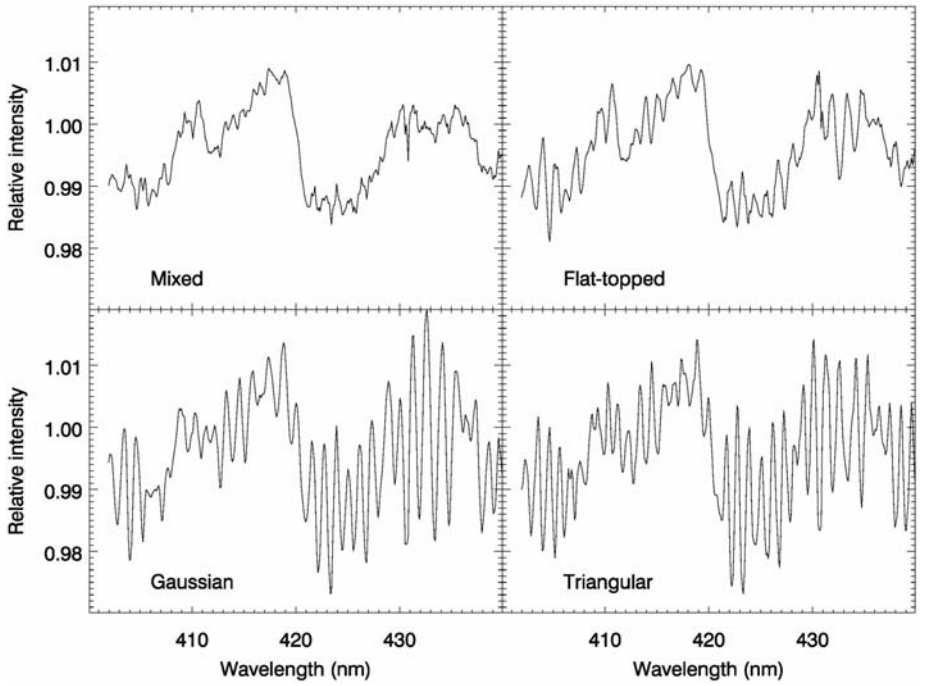

Figure 4 The effect of varying the shape of the slit function of the DOAS balloon low resolution reference spectrum (Gurlit *et al.*, 2005) used as a radiometric reference on Q^{losamp} (see text). A combination of a Gaussian and flat-topped shape gives the best result with the least high-frequency structure (top left).

ture yields the best spectral slit function for the lower resolution spectrum. The optimum slit function we found for the DOAS balloon spectrum was a combination of a Gaussian ($\exp(-(\lambda-\lambda_0)/a)^2$) and a more square profile shape ($\exp(-(\lambda-\lambda_0)/b)^4$) (called 'Mixed' in Figure 4). We found that the width of the spectral slit function varies slightly over the wavelength range. This variation in width with wavelength was also taken into account. The lower-frequency features that remain for the best spectral slit functions are subsequently used to modify the radiometric calibration of the high resolution reference spectrum. The results as shown in Figure 4 are representative for the complete wavelength range 250 – 550 nm.

3.4. Interpolation between High and Low Resolution Wavelength Grids

In the above-described steps 2 and 4, we rework the convolved high resolution spectrum ($F_{\text{lores}}^{\text{hisamp}}$) and the fractional spectrum (Q^{losamp}) respectively to a different wavelength grid. The first case is straightforward, since clearly the high resolution spectrum has a much higher spectral sampling than the low resolution spectrum, so interpolation errors are very small. The second step requires more attention. The fraction Q^{losamp} reflects the radiometric update to the original high resolution spectrum. However, this fraction contains errors. First, errors result from inaccuracies in the low resolution spectrum, such as the imperfect representation of the slit function and remaining wavelength calibration errors. The principle applied in determining the optimal wavelength calibration and low resolution slit function is examining the structure in Q^{losamp}. The procedure is illustrated in Figure 4, which shows

the effect that changing the slit function shape has on Q^{losamp}. The goal is to get a residual that is as smooth as possible. It can be seen that the assumed slit function shape strongly influences the structures in Q^{losamp}. The wavelength calibration of the low resolution spectrum also has an effect (not shown) on that part of the spectrum where the strong Fraunhofer lines are located, *e.g.*, around 410 and 430 nm. We attempt to minimize the high frequency residual, in particular outside the regions with strong Fraunhofer lines and by minimizing the residuals at the Fraunhofer lines, in order to find the optimal shape of the slit function and the optimal wavelength calibration. It was found that the optimal slit function (shape and width) and the wavelength calibration are not constant for all wavelengths.

A next step in deriving Q^{losamp} is to smooth the original structure. The idea behind this is that only the broad features are due to the inaccurate radiometric calibration of the original high resolution spectrum, but that the fine details are noisy residuals of the fitting process. In going from Q^{losamp} to Q^{hisamp} the former signal is interpolated using splines to the wavelength grid of the high resolution spectrum.

3.5. Uncertainty Contributions

The procedure described above of combining a radiometric reference spectrum with a high resolution spectrum contains a number of uncertainty contributions. The spectral resolution and the spectral calibration accuracy of the high resolution spectrum cannot be improved, except by new measurements. On the other hand, since we apply only broad band corrections these properties will not be affected. The wavelength calibration of the low resolution spectra was changed in order to minimize the fine structure in the 'relative difference spectrum' Q^{losamp}, but does not add to the overall uncertainty in the wavelength calibration of the high resolution spectrum presented in this paper.

The uncertainty in the absolute radiometric calibration is mainly determined by the uncertainty in the used low resolution reference spectra. From a detailed study by Thuillier *et al.* (2003) it was determined that for the wavelength range discussed in this paper the Root – Mean – Square (RMS) differences between a large number of low resolution solar reference spectra is approximately 2%. Thus, the absolute radiometric accuracy of the high resolution spectrum derived in the present document is also approximately 2%.

4. Results, Comparison and Verification

In this section we make a comparison between the newly derived high resolution solar reference spectrum and the two lower resolution solar spectra that were used for the radiometric calibration. Comparisons are also made to two solar spectra from the literature. In addition, we compare the result with solar spectra from both the SCIAMACHY mission (Weber, 2006) and the OMI mission. In order to make these comparisons, all spectra were convolved with a triangular slit function to obtain the same 2 nm resolution.

Figure 5 shows the ratio of the final result of the high resolution solar reference spectrum divided by the SUSIM (Floyd *et al.*, 2003) and balloon (Gurlit *et al.*, 2005) lower resolution solar reference spectra that were used for the radiometric calibration. The result should ideally be one, but it can be observed that some residual features with amplitudes of up to 2%, but mostly smaller than 1%, remain, because the lower spectral resolution correction factors we applied to the original high resolution spectrum do not correct for every observed spectral feature. The origin of these features is tentatively attributed in part to the SUSIM spectrum (mainly for the stronger Fraunhofer lines) and in part to the high resolution solar

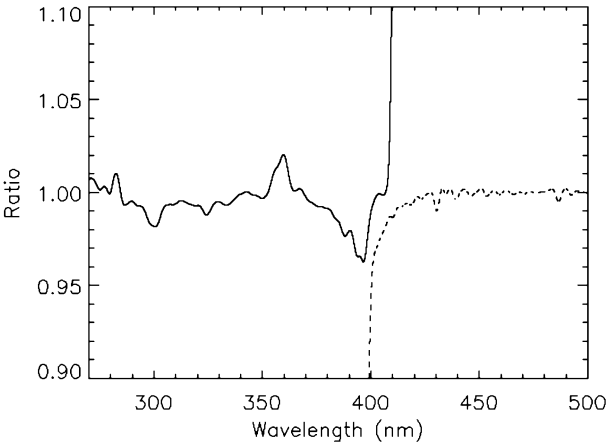

Figure 5 Ratio at 2 nm resolution of convolved high resolution solar reference spectrum as derived in this study divided by convolved lower resolution solar reference spectra in the UV and in the VIS wavelength ranges that were used to radiometrically calibrate the high resolution spectrum.

reference spectrum. The SUSIM lower resolution spectrum becomes less accurate towards 410 nm and the balloon lower resolution spectrum becomes less accurate towards 400 nm as a result of the decreasing instrument sensitivities towards these wavelengths. In the overlap region between the two spectra around 400 – 410 nm an optimized interpolation in the radiometric correction factors to the high resolution spectrum was performed.

In Figure 6 the percentage differences between our new reference spectrum and a number of other solar spectra, $100 \cdot (\frac{\text{new}-\text{other}}{\text{other}})$, each at the same 2 nm resolution, are shown. First the published reference spectra of Chance and Spurr (1997) and Thuillier *et al.* (2003) are considered. Discrepancies of more than 15% between our spectrum and the spectrum of Chance and Spurr (1997) can be observed, especially below 330 nm, which is as expected, because the Chance and Spurr spectrum was not radiometrically optimized for that wavelength region. Differences with the Thuillier *et al.* (2003) spectrum of up to about 5% can be seen. This is in line with the observation made by Thuillier *et al.* (2003) that the SOLSPEC irradiance is 3% to 4% higher than SUSIM irradiance. On top of some fine structure variations we observe an offset of 2% to 4% over the entire wavelength region, so this matches well with the difference between the SUSIM and SOLSPEC data as observed by Thuillier *et al.* (2003).

When considering the difference between the OMI spectrum and the new reference spectrum we need to keep in mind that the OMI absolute radiometric calibration was optimized using the newly derived reference spectrum. However, this adjustment included only small broad band structures. The correction factor is shown as the top curve in the bottom panel of Figure 6 with an offset of 15% for clarity in the figure. The agreement between the two spectra is within 2%. Only between 390 and 400 nm is the difference significantly larger than 1%. The reason for this is the presence of the strong Ca II H and K lines. Similar differences are observed in the other solar spectra. The Ca II H and K lines show a relatively strong variability, about a factor of 3 more than the local continuum. For the SCIAMACHY spectrum (not shown in Figure 6) above 350 nm the difference amounts to about 1%, but below 350 nm the difference gradually increases to 8%, with the SCIAMACHY spectrum being higher in that wavelength range. This is much better than the earlier reported uncertainty of 15% (Skupin *et al.*, 2002).

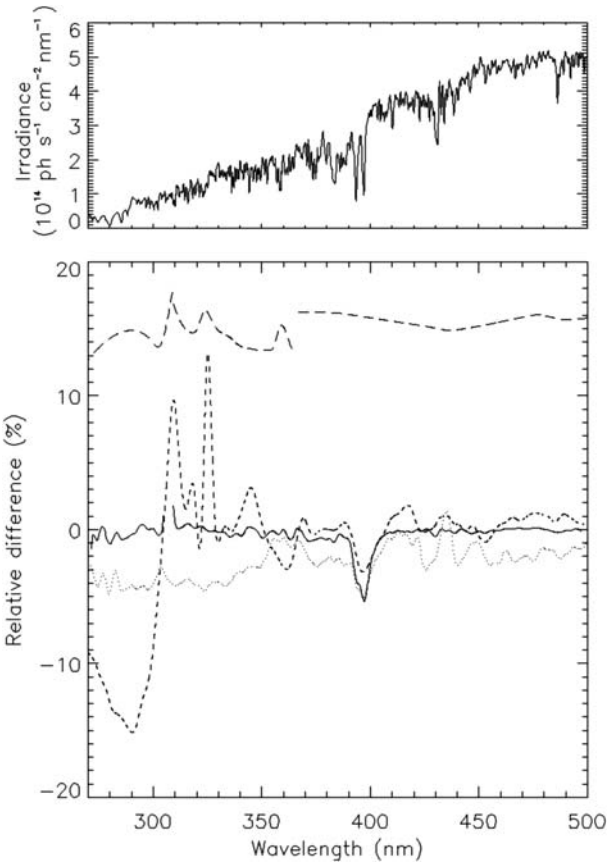

Figure 6 Bottom panel: Difference in percent of three solar spectra with the new solar reference spectrum at 2 nm resolution. The solid line is the comparison with the OMI measurement, the dotted line with Thuillier *et al.* (2003) and the dashed line with Chance and Spurr (1997). The radiometric update of the OMI calibration is also shown as the long-dashed line at the top in the bottom panel. This line has been shifted upwards by 15% for clarity. An OMI solar spectrum is shown in the top panel for comparison.

4.1. Variability of the Solar Spectrum

The Sun is a variable star. It varies on different timescales, ranging from seconds to days to years. The best known variation of the solar spectral irradiance is the 11 year solar cycle. Most of the spectral variability occurs at short wavelengths, *i.e.*, below 200 nm. From 11 years of SUSIM UARS measurements (Floyd *et al.*, 2003) it was found that between the Al edge (215 nm) and about 263 nm the solar cycle RMS variation is 3 – 4%. Above 263 nm the variation declines to approximately 1% at 300 nm. Thuillier *et al.* (2004) publish solar reference spectra for two different stages in the solar cycle (ranging from 200 to 2400 nm). However, in the present paper we are only concerned with the wavelength range between 250 and 550 nm, where the variability is mostly below 1%. Therefore we derive only one spectrum, which is valid for all stages in the 11 year solar cycle.

5. Conclusions

Based on previously published solar reference spectra we have constructed a new high resolution solar reference spectrum with both a high spectral and a radiometric accuracy in the range from 250 to 550 nm. After making small ($\sim 2\%$) spectrally broad adjustments to the

OMI radiometric calibration, the agreement with the OMI solar measurements is excellent (mostly within 2%). This indicates that the solar spectrum measured by OMI can be well reproduced by convolving the newly derived high resolution solar reference spectrum with the measured OMI slit functions. The only larger discrepancy remains at the Ca II H and K lines around 400 nm. We also find that the agreement on a 2 nm resolution grid with most other solar reference spectra is within 4 – 5%. The derived high resolution solar reference spectrum has an accurate radiometric scale over the entire wavelength range between 250 and 550 nm, as well as a high resolution (0.025 nm) and sampling (0.01 nm), with an accurate wavelength scale of better than 0.002 nm over the whole wavelength range.

Acknowledgements This research was funded by the Netherlands Agency for Aerospace Programmes (NIVR) within the framework of the Ozone Monitoring Instrument (OMI) project. We thank Dr. Mark Weber (IUP-Bremen) for providing us with the latest version of the SCIAMACHY solar spectrum. We also thank Dr. Aaron Lindner and Prof. Dr. Klaus Pfeilsticker (IUP-Heidelberg) for providing us with an improved version of the balloon spectrum used in the SCIAMACHY validation campaign.

References

Brueckner, G.E., Edlow, K.L., Floyd, L.E., Lean, J.L., VanHoosier, M.E.: 1993, *J. Geophys. Res.* **98**, 10695.
Burrows, J.P., Hoelzle, E., Goede, A.P.H., Visser, H., Fricke, W.: 1995, *Acta Astron.* **35**, 445.
Burrows, J.P., Weber, M., Buchwitz, M., Rozanov, V., Ladstätter-Weissenmayer, A., Richter, A., *et al.*: 1999, *J. Atmos. Sci.* **56**, 151.
Chance, K., Spurr, R.J.D.: 1997, *Appl. Opt.* **36**, 5224.
Dirksen, R., Dobber, M.R., Voors, R., Levelt, P.: 2006, *Appl. Opt.* **45**, 3972.
Dobber, M.R., Dirksen, R., Levelt, P., van den Oord, G.H.J., Voors, R., Kleipool, Q., Jaross, G., Kowalewski, M., Hilsenrath, E., Leppelmeier, G.W., de Vries, J., Dierssen, W., Rozemeijer, N.: 2006, *IEEE Trans. Geosci. Remote Sens.* **44**(5), 1209.
Floyd, L., Rottman, G., DeLand, M., Pap, J.: 2003. In: *Proc. ISCS 2003 Symposium "Solar Variability as an input to the Earth's Environment"* **SP-535**, ESA, Noordwijk, 195.
Gurlit, W., Bosch, H., Bovensmann, H., Burrows, J.P., Butz, A., Camy-Peyret, C., *et al.*: 2005, *Atmos. Chem. Phys.* **5**, 1879.
Hall, L.A., Anderson, G.P.: 1991, *J. Geophys. Res.* **96**, 12927.
Heath, D.F., Park, H.: 1978, In: Madrid, C.R. (ed.) *The Nimbus-7 Users Guide*, NASA Goddard Space Flight Center, Greenbelt, 175.
Kurucz, R.L.: 1995, In: Anderson, G.P. (ed.) *Proc. 17th Annual Conference Transmission Models*, 333.
Kurucz, R.L., Furenlid, I., Brault, J., Testerman, L.: 1984, *Solar Flux Atlas from 296 to 1300 nm*, National Solar Observatory, Sunspot. ftp://ftp.noao.edu/fts/fluxatl.
Kurucz, R.L., Bell, B.: 1995, *CD-ROM No. 23—Atomic Line List*, Smithonian Astrophysical Observatory, Cambridge.
Levelt, P.F., van den Oord, G.H.J., Dobber, M.R., Mälkki, A., Visser, H., de Vries, J., Stammes, P., Lundell, J.O.V., Saari, H.: 2006a, *IEEE Trans. Geosci. Remote Sens.* **44**(5), 1093.
Levelt, P.F., Hilsenrath, E., Leppelmeier, G.W., van den Oord, G.H.J., Bhartia, P.K., Tamminen, J., de Haan, J.F., Veefkind, J.P.: 2006b, *IEEE Trans. Geosci. Remote Sens.* **44**(5), 1199.
Schoeberl, M.R., Douglass, A.R., Hilsenrath, E., Bhartia, P.K., Beer, R., Waters, J.W., *et al.*: 2006, *IEEE Trans. Geosci. Remote Sens.* **44**(5), 1066.
Skupin, J., Noel, S., Wuttke, M.W., Bovensmann, H., Burrows, J.P.: 2002, In: *Proc. of the Envisat Validation Workshop* **SP-531**, ESA, Noordwijk.
Thuillier, G., Hersé, M., Simon, P., Labs, D., Mandel, H., Gillotay, D.: 1997, *Solar Phys.* **171**, 283.
Thuillier, G., Hersé, M., Simon, P., Labs, D., Mandel, H., Gillotay, D., Foujols, T.: 1998, *Solar Phys.* **177**, 41.
Thuillier, G., Hersé, M., Labs, D., Foujols, T., Peetermans, W., Gillotay, D., Simon, P., Mandel, H.: 2003, *Solar Phys.* **214**, 1.
Thuillier, G., Floyd, L., Woods, T.N., Cebula, R., Hilsenrath, E., Hersé, M., Labs, D.: 2004, *Adv. Space Res.* **34**, 256.
Weber, M.: 2006, Private Communication.
Woods, T.N., Prinz, D.K., Rottman, G.J., London, J., Crane, P.C., Cebula, R.P., Hilsenrath, E., *et al.*: 1996, *J. Geophys. Res.* **101**, 9541.